Planning High-quality Paths and Corridors Amidst Obstacles*

Ron Wein
School of Computer Science
Tel Aviv University
Israel
wein@tau.ac.il

Jur van den Berg
Department of Computer Science
University of North Carolina at Chapel Hill
USA
berg@cs.unc.edu

Dan Halperin
School of Computer Science
Tel Aviv University
Israel
danha@tau.ac.il

Abstract

The motion-planning problem, involving the computation of a collision-free path for a moving entity amidst obstacles, is a central problem in fields such robotics and game design. In this paper we study the problem of planning high-quality paths. A high-quality path should have some desirable properties: it should be short*, avoiding long detours, and at the same time it should stay at a safe distance from the obstacles, namely it should have* clearance*. We suggest a quality measure for paths, which balances between the above criteria of minimizing the path length while maximizing its clearance. We analyze the properties of optimal paths according to our measure, and devise an approximation algorithm to compute near-optimal paths amidst polygonal obstacles in the plane. We also apply our quality measure to corridors. Instead of planning a one-dimensional motion path for a moving entity, it is often more convenient to let the entity move in a* corridor*, where the exact motion path is determined by a local planner. We show that planning an optimal corridor is equivalent to planning an optimal path with* bounded *clearance.*

KEY WORDS—Motion planning, bi-criteria optimization, corridors

The International Journal of Robotics Research
Vol. 27, No. 11–12, November/December 2008, pp. 1213–1231
DOI: 10.1177/0278364908097213

Figures 1–13 appear in color online: http://ijr.sagepub.com

1. Introduction

1.1. Optimal Paths

The task of planning a collision-free path for a moving entity that avoids obstacles plays an important role in robotics, as well as in game design. The problem is often solved by constructing a graph that discretizes the environment, and extracting a collision-free path from this graph. The nodes of such a graph may be the cells of a uniform grid (see, e.g., Russel and Norvig (2002)) or, according to the probabilistic roadmap (PRM) paradigm (see Kavraki et al. (1996) and Choset et al. (2005, Chapter 7)), free configurations that are chosen randomly, attempting to capture the connectivity of the free configuration space. Alternatively, in exact algorithmic solutions, the nodes of the so-called connectivity graph correspond to the cells of the exact decomposition of the free space (see, e.g., Latombe (1991); Sharir (2004)).

In many applications, computing *some* collision-free path is not enough, and we are required to obtain a high-quality path. The quality of a path can be determined according to several properties. Usually, a preferable path is short, avoiding unnecessary detours. At the same time, the path is often required to have some clearance from the obstacles, in order to allow the moving entity more room to maneuver safely, or to gain

* A preliminary version of this paper appeared in *Proceedings of the 7th International Workshop on the Algorithmic Foundations of Robotics (WAFR)*, New York, July 2006.

increased visibility. Song et al. (2001) present a method for extracting paths from a PRM according to these criteria. Additional path properties of interest are the path smoothness or, more generally, the amount of curvature a path has.

Paths extracted from a PRM are usually piecewise linear, thus containing sharp turns, and possibly also self-loops. To be of practical use, such paths need to be postprocessed. Here lies a major drawback of the above approaches: they may select a path which is optimal according to some quality measure *within the graph*, yet other paths may exist in the graph that may prove better after they are postprocessed. Trying all paths and only selecting the best one after postprocessing would be prohibitively expensive.

In this paper we consider the problem of characterizing and computing high-quality motion paths. This problem is also closely related to the problem of routing thick paths, as studied by Mitchell and Polishchuk (2007). As we have already mentioned, this is a bi-criteria optimization problem, as we strive for minimizing the path length while maximizing its clearance for the given obstacles. These two requirements are often contradictory. Given start and goal configurations and a set of obstacles in the plane, the shortest collision-free path is contained in the *visibility graph* of the obstacles; see, e.g., Mitchell (2004). However, such a path is incident to obstacle boundaries and therefore has zero clearance. Conversely, if one is only concerned with clearance, allowing as long paths as needed, then such paths are easily found by retracting the path to the *Voronoi diagram* of the given obstacles (Ó'Dúnlaing and Yap 1985). It is also possible to consider interpolations of these two structures, named *visibility–Voronoi diagrams*, as we suggested in Wein et al. (2007). Indeed, a good path makes a good trade-off between length and clearance.

Our work on the visibility–Voronoi diagram still falls short of precisely quantifying the tradeoff between the length and clearance of paths. In this paper we introduce a measure for the quality of paths, which combines the two properties mentioned above, path length and path clearance, and presents a method to plan paths amidst polygonal obstacles in the plane that are (nearly) optimal with respect to this measure. In addition, we show that such optimal paths are always smooth.

Planning optimal paths with respect to our quality measure is a computationally difficult task. However, we show how to devise optimal paths in some special cases, and devise an approximation algorithm that computes near-optimal paths amidst polygonal obstacles.

1.2. Optimal Corridors

Computing a fixed path in response to a motion-planning query is inadequate for many applications, as such a path lacks flexibility to avoid local hazards (such as small obstacles, other moving entities, etc.) that are encountered during the motion. Moving along a fixed path also leads to predictable, and possibly unrealistic motions, which are not suitable for some applications, such as computer games. One approach for tackling these problems is a potential-field planner, in which the moving entity is attracted to its goal configuration, and repelled by obstacles, or other moving entities (see, e.g., Khatib (1986)). However, this approach is prone to get stuck in local minima of the potential field. Although there are methods that help in getting out of local minima (see, e.g., Latombe (1991, Chapter 7)), they may still not yield valid motions at all, even when valid paths exist.

We would therefore like to indicate the global direction of movement for the moving entity, while leaving enough flexibility for some *local planner* to avoid local hazards. An ideal solution for this is to use *corridors*, which have recently been introduced in the field of game design; see Overmars (2005). Corridors are defined as a union of balls whose center points lie along a backbone path. The radius of the balls is determined by the *clearance* (i.e. the distance to the nearest obstacle) along the backbone path. The more restricted task of locally planning the motion around the backbone path can be successfully performed by applying potential-field methods within the corridor. At the same time, in order to guarantee that the local planner operates on a restricted environment, the radii of the balls are upper bounded by some predetermined value[1]. As a result, rather than moving along a fixed path, the moving entity moves within a corridor around the backbone path. This gives a strict global direction of movement, yet provides the local flexibility we look for.

Planning within corridors has many applications. It has been used to plan motions for coherent groups of entities, where the backbone path provides the global motion of the group (Kamphuis and Overmars 2004). The interactions between entities of the group are locally controlled by a social potential-field method (Reif and Wang 1995). Corridors have also been used to plan the motion of a camera that follows a moving character (a *guide*) (Nieuwenhuisen and Overmars 2004a). If the guide moves along the backbone path, the corridor gives the flexibility for the camera to swerve if necessary. Another advantage of corridors is that they allow for nonholonomic and kinodynamic planning, if the motion of a single entity (or multiple entities) is planned using a potential field method within the corridor (Kamphuis et al. 2005). This is very difficult to achieve and incorporate into a fixed path. A common property of the applications of corridors is that the moving entity is small compared with the scale of the environment. In many fields (open field robotic navigation, games, etc.) this is indeed the case.

We show that planning an optimal corridor is equivalent to computing an optimal path with bounded clearance. We are therefore able to generalize our analysis to corridors and plan near-optimal corridors amidst polygonal obstacles.

1. The fact that the radii of the balls are bounded is a major difference between a corridor and the *medial axis transform* of the free workspace.

1.3. Paper Outline

The rest of this paper is organized as follows. In Section 2 we formally define a quality measure for paths and present some elementary properties of general optimal paths with respect to this measure. Section 3 focuses on the specific case of optimal paths amidst polygonal obstacles in the plane and discusses their properties. In Section 4 we present an approximation algorithm to compute near-optimal paths. In Section 5 we generalize our result to the case of corridors. We also take the curvature of the path into account and augment the quality measure accordingly. We give some concluding remarks and future-work directions in Section 6.

2. Measuring Paths

In this section, we formally define what a path is, and how we measure its quality. We show properties of paths that are optimal with respect to this measure, namely that an optimal path is smooth, and that it obeys Snell's law of refraction when the clearance function plays the role of the "speed of light".

2.1. Paths

A *path* $\gamma(t)$ of an entity moving in a d-dimensional workspace is defined as a continuous function $\gamma : [0, L] \longrightarrow \mathbb{R}^d$, parameterized by the length L of the path. In typical motion-planning applications we are given a set of obstacles $\mathcal{O}$ that the moving entity should avoid. If there exists some $t \in [0, L]$ such that the interior of the moving entity intersects some obstacle when positioned at $\gamma(t)$, we say that γ is an invalid path. For the time being, let us assume that the moving entity is a point; thus, it is sufficient to require that γ is disjoint from the interior of any of the obstacles. In the following sections we explain how it is possible to avoid this assumption. In the rest of this paper we consider only valid, namely collision-free, paths.

For any point p, we define the *clearance* as a function $c : \mathbb{R}^d \longrightarrow \mathbb{R}$, where $c(p)$ is the distance between p and the nearest point on any of the obstacles. That is, $c(p) = \min_{q \in \mathcal{O}} \|p - q\|$.

2.2. The Weighted Length Measure

As we have already indicated, a good path must be short, namely it should avoid unnecessarily long detours, and it should have as much clearance as possible. Informally speaking, the path should go through narrow passages only if they allow considerable shortcuts.

To combine the two desired properties of the path as discussed above, for any $\delta > 0$ we define the *weighted length* $L^*_\delta(\gamma)$ of a path γ to be

$$L^*_\delta(\gamma) = \int_\gamma \left(\frac{1}{c(\gamma(t))}\right)^\delta dt. \tag{1}$$

We wish to minimize the weighted length by either shortening the path or by extending the path's clearance. Given a start position $s \in \mathbb{R}^d$ and a goal position $g \in \mathbb{R}^d$, a path γ satisfying $\gamma(0) = s$ and $\gamma(L) = g$ is *optimal* for a desired value of δ if for any other valid path γ' connecting the two endpoints we have $L^*_\delta(\gamma) \leq L^*_\delta(\gamma')$.

The parameter δ determines how much weight is given to the clearance in the measure. That is, if δ is small, the length is more important than the clearance, and if δ is large, the clearance is more important than the length. Indeed, if $\delta = 0$, the weighted length equals the length of the path, and the optimal path is the shortest path. In the plane, the shortest path is contained in the visibility graph of the obstacles $\mathcal{O}$. This graph can be computed in $O(n \log n + k)$ time (Mitchell 2004), where n is the total complexity of the obstacles, and k the number of edges in the visibility graph. For $\delta \longrightarrow \infty$, the optimal path is the path with the largest minimal clearance in the Voronoi diagram of the obstacles $\mathcal{O}$. It can be found in $O(n \log n)$ time by *retraction*, namely by constructing a minimum spanning tree in the Voronoi diagram (Ó'Dúnlaing and Yap 1985).

Our weighting scheme can be applied directly to optimizing the quality of paths extracted from PRMs that contain cycles, as suggested by Nieuwenhuisen et al. (2004) and Nieuwenhuisen and Overmars (2004b). In this case, instead of weighting each edge in the PRM by its Euclidean length and extracting the shortest path from the graph, we can consider some preferred δ value, and give each edge e the weight of $L^*_\delta(e)$, with respect to the clearance function along the edge. We can thus extract the optimal path the PRM contains with respect to δ. However, for polygonal obstacles in the plane we can devise a complete scheme for calculating an optimal path, as we show in the next section.

2.3. Properties of Optimal Paths

Observation 1. *The clearance function $c(\gamma(t))$ is a continuous function along any path γ. Moreover, for any $p_1, p_2 \in \mathbb{R}^d$ we have $|c(p_2) - c(p_1)| \leq \|p_2 - p_1\|$, hence the clearance function also satisfies the Lipschitz condition with a constant that equals* 1.

Lemma 2. *Given a set of obstacles and $0 < \delta < \infty$, an optimal path connecting any given start position s to any goal position g is smooth.*

Proof. Let $\gamma(t)$ be an optimal path connecting s and g. Assume that γ contains a sharp turn (a $\mathcal{C}_1$-discontinuity). Let us approximate the sharp turn using a circular arc of radius r that connects smoothly to the original path. As illustrated in Figure 1, as r approaches 0 the approximation is tighter. Let ℓ_1 be

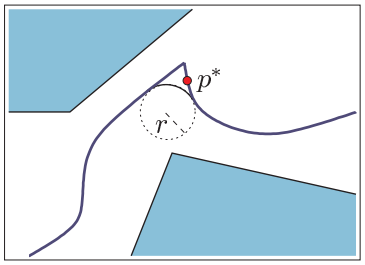

Fig. 1. Shortcutting a path segment that contains a sharp turn using a smooth circular arc.

the length of the original path segment we approximate, and let ℓ_2 be the length of the circular arc. It is easy to show that there exists $\hat{r} > 0$ and some constants $A_1 > A_2 > 0$ such that for each $0 < r < \hat{r}$ we have $\ell_1 \geq A_1 r$ and $\ell_2 = A_2 r$. If the maximal clearance c^* along the original path segment is attained at some point p^*, then as the distance of any point p along the circular arc from p^* is bounded by Kr, where K is some constant, and as the clearance function is 1-Lipschitz, we have that $c^* - c(p) < Kr$. Let L_1^* be the weighted length of the original path segment and let L_2^* be the weighted length of the circular arc. We therefore know that $L_1^* \geq (1/c^*)^\delta \cdot l_1$ and $L_2^* \leq (1/(c^* - Kr))^\delta \cdot l_2$, so we can write

$$\frac{L_1^*}{L_2^*} \geq \frac{(1/c^*)^\delta \cdot l_1}{(1/(c^* - Kr))^\delta \cdot l_2} \geq \left(\frac{c^* - Kr}{c^*}\right)^\delta \cdot \frac{A_1}{A_2}.$$

As $A_1 > A_2$, we can choose

$$0 < r < \min\left\{\frac{c^*}{K}\left(1 - \sqrt[\delta]{\frac{A_2}{A_1}}\right), \hat{r}\right\}$$

such that the entire expression above is greater than one. We thus have $L_1^* > L_2^*$, and we managed to decrease the weighted length of the original path by introducing a circular shortcut, in contradiction to the optimality of γ. We conclude that $\gamma(t)$ must be a smooth function. ■

It is clear that in the case of a constant clearance function, the optimal path between two points is a straight-line segment. We therefore use infinitesimal analysis at several places in this paper, treating the clearance function as being piecewise constant, and approximate optimal path between two points by polylines. To this end, we need to examine the nature of optimal paths with respect to a non-continuous clearance function.

Assume that we have some hyperplane $\mathcal{H}$ in $\mathbb{R}^d$ that separates two regions, such that in one region the clearance is c_1 and in the second it is c_2. Minimizing the weighted length between two endpoints that are separated by $\mathcal{H}$ is equivalent to applying Fermat's principle, stating that the actual path between two points taken by a beam of light is the one that is traversed in the least time. The optimal path thus crosses the separating hyperplane once, such that the angles α_1 and α_2 it forms with the normal to $\mathcal{H}$ obey Snell's Law of refraction[2], with ${c_1}^\delta$ and ${c_2}^\delta$ playing the role of the "speed of light" in the respective regions. We omit the proof of the following lemma, as it is identical to the usual Snell's law of optimality in the weighted regions problem (see Mitchell and Papadimitriou (1991)).

Lemma 3. (Snell's law of refraction) *Consider two regions separated by the line $y = 0$, such that if our path is given by $\gamma(t) = (x(t), y(t))$, then $c(\gamma(t)) = c_1$ for $y(t) \geq 0$ and $c(\gamma(t)) = c_2$ for $y(t) < 0$. The angles α_1 and α_2 that the optimal path between $p_1 = (x_1, y_1)$ and $p_2 = (x_2, y_2)$, where $y_1 > 0$ and $y_2 < 0$, forms with a vertical line perpendicular to $y = 0$ satisfy*

$${c_2}^\delta \sin\alpha_1 = {c_1}^\delta \sin\alpha_2. \tag{2}$$

3. Optimal Paths Amidst Polygonal Obstacles in the Plane

In this section, we consider planar environments cluttered with polygonal obstacles. We show that the behavior of an optimal path is determined by the identity of the nearest obstacle feature, which is either a polygon vertex (or a point obstacle), or a polygon edge (or a line obstacle): we show that an optimal path is a *logarithmic spiral* in the vicinity of a point obstacle, and a *circular arc* in the vicinity of a line obstacle. Based on these results, we show that an optimal path consists of a bounded number of segments whose identity is determined by the cell of the *Voronoi diagram* of the polygons the path is in. We also show that an optimal path can lie on an arc of this Voronoi diagram. We also show how to compute the weighted length of each type of path segment.

From now on, we assume that $\delta = 1$, which gives a natural trade-off between length and clearance in two-dimensional environments, and for which we can analytically express the structure of an optimal path. The choice of $\delta = 1$ will become more natural when we introduce corridors in Section 5 and focus on planning optimal backbone paths for corridors. To simplify the notation, we refer to $L_1^*(\cdot)$ simply as $L^*(\cdot)$. We mention that the analysis for arbitrary values of δ is performed using calculus of variations; see, e.g., Gelfand and Fomin (2000). In Appendix A we give more details on the techniques we use in the general case.

3.1. A Single Point Obstacle

Let us assume that there is only a single point obstacle p in our environment. Without loss of generality, we assume that p

2. See also Mitchell and Papadimitriou (1991), where this observation is used in a similar setting of the problem.

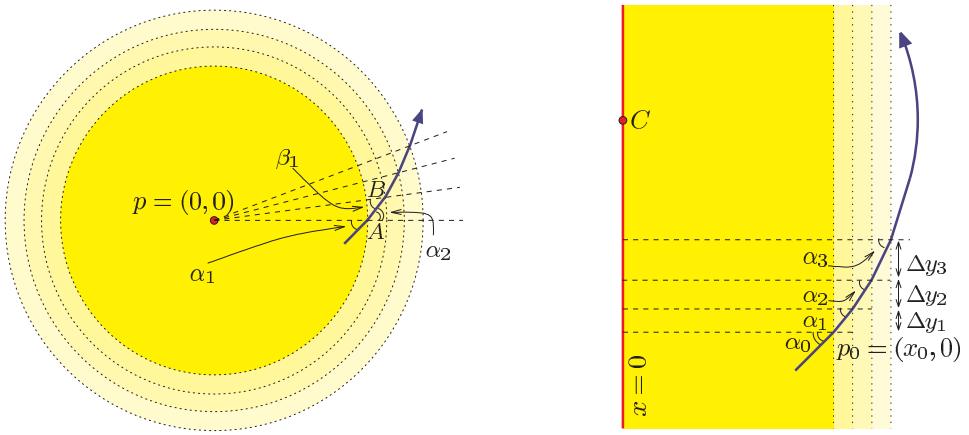

Fig. 2. An optimal path in the case of (a) a single point obstacle and (b) a single line segment obstacle.

is located at the origin. We show how to compute an optimal path between two endpoints $s, g \in \mathbb{R}^2$. Note that the clearance $c(\gamma(t))$ along such a path simply is equal to $\|\gamma(t)\|$.

We first approximate the optimal path by a polyline: for some small $\Delta r > 0$, we look at the circles of radii $\Delta r, 2\Delta r, 3\Delta r, \ldots$ that are centered at the origin. Each pair of neighboring circles define an annulus. Since Δr is small we assume that the distance from p of all points in the kth annulus is constant and equal to $k\Delta r$. Consider the scenario depicted in Figure 2(a), where γ enters one of the annuli at some point A, where $\|A\| = r_1$, and leaves this annulus at B, where $\|B\| = r_2 = r_1 + \Delta r$. The angles that the path forms with pA and pB are α_1 and β_1, respectively. When entering the annulus we have $c_1 = r_1$ and $c_2 = r_2$, so applying Equation (2) for $\delta = 1$ we can express the refracted angle α_2, using

$$\sin\alpha_2 = \frac{r_2}{r_1}\sin\alpha_1.$$

By applying the law of sines on the triangle $\triangle pAB$, we obtain

$$\frac{r_2}{\sin(\pi - \alpha_2)} = \frac{r_1}{\sin\beta_1},$$

$$\sin\beta_1 = \frac{r_1}{r_2}\sin(\pi - \alpha_2) = \frac{r_1}{r_2}\sin\alpha_2 = \sin\alpha_1.$$

As the two angles are less than $\pi/2$, we have that $\beta_1 = \alpha_1$. Taking $\Delta r \longrightarrow 0$, we obtain a smooth curve γ, such that the angle that $\nabla\gamma(t)$ forms with $\overrightarrow{p\gamma(t)}$ is a constant ψ. It is possible to show that a curve that has this property must be a segment of a *logarithmic spiral* (also called an *equiangular spiral*) whose polar equation is given by $r(t) = ae^{b\theta(t)}$, where a is a constant and $b = \cot\psi$. See, e.g., Gray (1997) for a proof of this latter fact.

The two parameters a and b of the logarithmic spiral that support the optimal path between two given endpoints can therefore be computed by substituting the polar coordinates of the endpoints into the equation $r = ae^{b\theta}$:

Proposition 4. *Given a single point obstacle located at the origin, a start position $s = r_s e^{i\theta_s}$ and a goal position $g = r_g e^{i\theta_g}$ (in polar coordinates), the optimal path connecting s and g is a spiral arc supported by a logarithmic spiral $r = a^* e^{b^*\theta}$. Since both s and g lie on this spiral, we have (assuming $\theta_s \neq \theta_g$, otherwise the optimal path is simply a line segment):*

$$a^* = r_g^{\theta_s/(\theta_s-\theta_g)} \cdot r_s^{-\theta_g/(\theta_s-\theta_g)}, \tag{3}$$

$$b^* = \frac{1}{\theta_g - \theta_s} \cdot \ln\frac{r_g}{r_s}. \tag{4}$$

Proposition 5. *Given a single point obstacle located at the origin, a start position $s = r_s e^{i\theta_s}$ and a goal position $g = r_g e^{i\theta_g}$ (in polar coordinates), the weighted length of the optimal path σ between s and g is given by*

$$\begin{aligned} L^*(\sigma) &= \int_{\theta_1}^{\theta_2} \frac{1}{r(\theta)}\sqrt{r^2(\theta) + \left(\frac{dr}{d\theta}\right)^2(\theta)}\,d\theta \\ &= \int_{\theta_1}^{\theta_2} \frac{1}{a^* e^{b^*\theta}}\sqrt{1+b^{*2}}\,ae^{b^*\theta}\,d\theta \\ &= \int_{\theta_1}^{\theta_2} \sqrt{1+b^{*2}}\,d\theta = \sqrt{1+b^{*2}}(\theta_2 - \theta_1) \\ &= \sqrt{(\theta_2-\theta_1)^2 + (\ln r_2 - \ln r_1)^2}. \end{aligned} \tag{5}$$

3.2. A Single Line Segment Obstacle

Let us now consider an environment that consists of a single line segment obstacle, which is arbitrarily long. Without loss

of generality, let us assume that the segment is supported by the vertical line $x = 0$, such that the clearance of a point along the path $\gamma(t) = (x(t), y(t))$ simply equals $c(\gamma(t)) = |x(t)|$. To analyze the optimal path γ between two points s and g (see Figure 2(b)), we begin by approximating this path using a polyline. Assume that $\gamma(t)$ passes through a point $p_0 = (x_0, 0)$ and forms an angle α_0 with the line $y = 0$ perpendicular to the obstacle. For some small $\Delta x > 0$ we can define the lines $x = x_0, x = x_0 + \Delta x, x = x_0 + 2\Delta x, \ldots$, where each pair of neighboring lines define a vertical slab. Since Δx is small we assume that the distance of all points in the slab from the obstacle is constant and equal to $x_0 + k\Delta x$. We can now use Equation (2) with $\delta = 1$ and write

$$\begin{aligned}
\sin\alpha_1 &= \frac{x_0 + \Delta x}{x_0}\sin\alpha_0,\\
\sin\alpha_2 &= \frac{x_0 + 2\Delta x}{x_0 + \Delta x}\sin\alpha_1 = \frac{x_0 + 2\Delta x}{x_0}\sin\alpha_0,\\
&\vdots\\
\sin\alpha_k &= \frac{x_0 + k\Delta x}{x_0}\sin\alpha_0.
\end{aligned}$$

If we examine the kth slab we can write $x = x_0 + k\Delta x$, so we have

$$\begin{aligned}
\Delta y_k &= \Delta x \tan\alpha_k = \Delta x \cdot \frac{\sin\alpha_k}{\sqrt{1 - \sin^2\alpha_k}}\\
&= \Delta x \cdot \frac{x\sin\alpha_0}{\sqrt{x_0^2 - x^2\sin^2\alpha_0}}. \qquad (6)
\end{aligned}$$

Letting Δx tend to zero we obtain a smooth curve. We can use Equation (6) to express the derivative of the curve and we obtain

$$\begin{aligned}
y'(x) &= \lim_{\Delta x \to 0}\frac{\Delta y_k}{\Delta x} = \frac{x\sin\alpha_0}{\sqrt{x_0^2 - x^2\sin^2\alpha_0}},\\
y(x) &= -\frac{1}{\sin\alpha_0}\sqrt{x_0^2 - x^2\sin^2\alpha_0} + K. \qquad (7)
\end{aligned}$$

As the point $(x_0, 0)$ lies on the curve we can express the constant K:

$$\begin{aligned}
K &= 0 + \frac{1}{\sin\alpha_0}\sqrt{x_0^2 - x_0^2\sin^2\alpha_0}\\
&= \frac{\sqrt{1 - \sin^2\alpha_0}}{\sin\alpha_0}x_0 = x_0\cot\alpha_0.
\end{aligned}$$

Observe that $y(x)$ is defined only for $x < x_0/\sin\alpha_0$. When $x = x_0/\sin\alpha_0$ the path is reflected from the vertical wall and starts approaching the obstacle. Indeed, by squaring and rearranging Equation (7) we obtain

$$x^2 + (y - x_0\cot\alpha_0)^2 = \left(\frac{x_0}{\sin\alpha_0}\right)^2,$$

thus we conclude that γ is a circular arc, whose supporting circle is centered at $(0, x_0\cot\alpha_0)$ and its radius is $x_0/\sin\alpha_0$.

Proposition 6. *Given a start position $s = (x_s, y_s)$ and a goal position $g = (x_g, y_g)$ in the vicinity of a line segment obstacle supported by $x = 0$, the optimal path between these two endpoints is a circular arc supported by the a circle of radius r^* that is centered at $(0, y^*)$, where (we assume that $y_s \neq y_g$, otherwise the optimal path is simply the line segment sg):*

$$y^* = \frac{y_s + y_g}{2} + \frac{x_g^2 - x_s^2}{2(y_g - y_s)}, \qquad (8)$$

$$r^* = \sqrt{\frac{1}{2}(x_s^2 + x_g^2) + \frac{1}{4}(y_g - y_s)^2 + \frac{(x_g^2 - x_s^2)^2}{4(y_g - y_s)^2}}. \qquad (9)$$

Proposition 7. *Given a line segment obstacle supported by the line $x = 0$, a start position $s = r^*e^{i\theta_1}$ and a goal position $g = r^*e^{i\theta_2}$ in polar coordinates relative to the center $(0, y^*)$ of the circle supporting the optimal path σ between s and g, the weighted length of the circular arc σ is given by (note that $r(\theta) = r^*$)*

$$\begin{aligned}
L^*(\sigma) &= \int_{\theta_1}^{\theta_2}\frac{1}{r^*\cos\theta}\sqrt{r^2(\theta) + \left(\frac{dr}{d\theta}\right)^2(\theta)}\,d\theta\\
&= \int_{\theta_1}^{\theta_2}\frac{1}{\cos\theta}\,d\theta = \ln\frac{1 + \sin\theta}{\cos\theta}\Bigg|_{\theta_1}^{\theta_2}\\
&= \ln\tan\frac{\theta_2}{2} - \ln\tan\frac{\theta_1}{2}. \qquad (10)
\end{aligned}$$

(The last transition is due to the half-angle formula $\tan(\varphi/2) = (1 + \sin\varphi)/\cos\varphi$.)

3.3. Polygonal Obstacles

For the general case of multiple polygonal obstacles, we first construct $\mathcal{V}$, the *Voronoi diagram* of the obstacle polygons. $\mathcal{V}$ consists of Voronoi arcs that are equidistant to two different polygon features. A Voronoi arc may be induced by two polygon vertices, by two polygon edges, or by a polygon vertex and a polygon edge that are adjacent on the same polygon, in which case it is a line segment, or by a polygon vertex and a polygon edge of different polygons, in which case it is a parabolic arc. See, e.g., Lee and Drysdale (1981) for more details.

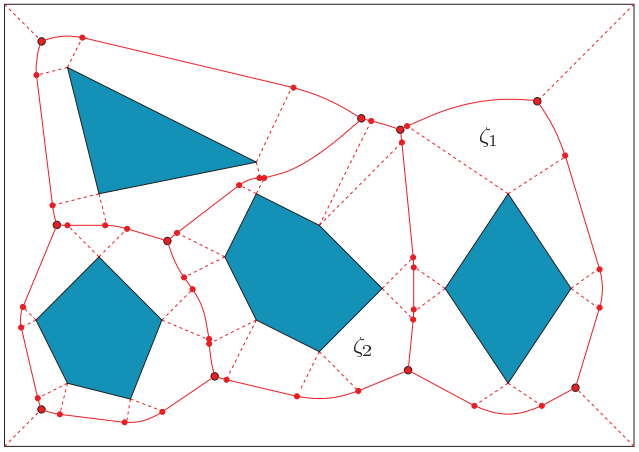

Fig. 3. The Voronoi diagram of four polygonal obstacles. Voronoi arcs separating between Voronoi cells of features of different polygons are drawn as solid lines and those separating cells of features of the same polygon are dashed lines. The region denoted ζ_1 is the Voronoi cell of a polygon vertex and ζ_2 is the Voronoi cell of a polygon edge.

The Voronoi arcs partition the plane into two-dimensional *Voronoi cells*, where all points in a cell share the same closest polygon feature. The closest polygon feature is either a polygon vertex, or a polygon edge. See Figure 3 for an illustration.

Given two points s' and g' that belong to the same Voronoi cell ζ, we know the following facts.

- If ζ is a Voronoi cell of a polygon *vertex*, the optimal path between s' and g' is a spiral arc σ that connects them as in Proposition 4, provided that σ does not intersect any Voronoi arc of $\mathcal{V}$. The weighted length of σ can be computed according to Proposition 5.
- If ζ is a Voronoi cell of a polygon *edge*, the optimal path between s' and g' is a circular arc σ that connects them as in Proposition 6, provided that σ does not intersect any Voronoi arc of $\mathcal{V}$. The weighted length of σ can be computed according to Proposition 7.

In addition, the Voronoi arcs of $\mathcal{V}$ are also *locally optimal*, namely they can serve as optimal paths. Given s' and g' on the same Voronoi arc, the optimal path that connects them is simply the piece of the Voronoi arc between s' and g'. In the case of a Voronoi arc that is induced by two polygon vertices or by two polygon edges, this is easy to prove: the Voronoi arcs are straight-line segments and the clearance function is locally maximal on the Voronoi arcs. The case of a Voronoi arc induced by a polygon vertex and a polygon edge that are adjacent on the same polygon reduces to the case in Proposition 4 where $\theta_{s'} = \theta_{g'}$ or, equivalently, to the case in Proposition 6 where $y_{s'} = y_{g'}$. Hence, these arcs are locally optimal as well.

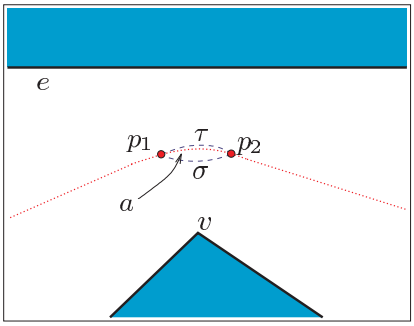

Fig. 4. A parabolic Voronoi arc a induced by a polygon vertex v and an edge e of another polygon, with p_1 and p_2 two points on a.

The case of a parabolic Voronoi arc induced by a polygon vertex and a polygon edge of different polygons is less trivial. To prove local optimality, we show that it is not possible to shortcut a piece of the arc between two points on the parabolic arc by choosing a shorter route that is closer to one of the polygons, as such a route always has a greater weighted length.

Consider a parabolic Voronoi arc a induced by a polygon vertex v and an edge e of another polygon, and let p_1 and p_2 be two points on a. Assume that it is possible to shortcut the portion of a defined by p_1 and p_2 by penetrating the Voronoi cell of e. In this case, the shortcut is a circular arc σ centered at some point on e; this arc clearly penetrates the Voronoi cell of the vertex v, as can be seen in Figure 4. On the other hand, if we try to create a shortcut contained in the Voronoi cell of v, we end up with a spiral arc τ centered at v. As p_1 and p_2 are equidistant from v, τ is a circular arc, whose curvature is greater than that of the parabolic edge, hence it penetrates the Voronoi cell of e. Either way, we reach a contradiction, and we conclude that the parabolic arc is locally optimal.

Corollary 8. *The optimal path between two points s' and g' on a Voronoi arc a of any kind is the piece of a between s' and g'.*

The weighted length of these paths is computed as follows.

- *Vertex–vertex arc.* Without loss of generality, let the two polygon vertices inducing the Voronoi arc a be the points $(0, y_v)$ and $(0, -y_v)$. Then, the Voronoi arc a is supported by the line $y = 0$, and the clearance for any point $(x, 0)$ along a is equal to $\sqrt{x^2 + {y_v}^2}$. The weighted length of the optimal path σ between to points $(x_1, 0)$ and $(x_2, 0)$ on a is equal to

$$L^*(\sigma) = \int_{x_1}^{x_2} \frac{1}{\sqrt{x^2 + {y_v}^2}}\, dx$$

$$= \ln\left(x + \sqrt{x^2 + {y_v}^2}\right)\Big|_{x_1}^{x_2}$$

$$= \ln \frac{x_2 + \sqrt{x_2^2 + {y_v}^2}}{x_1 + \sqrt{x_1^2 + {y_v}^2}}. \quad (11)$$

- *Edge–edge arc*. Without loss of generality, let the two polygon edges inducing the Voronoi arc a intersect the line $y = 0$ at the origin with angles α and $-\alpha$. Then, the Voronoi arc a is supported by the line $y = 0$, and the clearance for any point $(x, 0)$ along a equals $x \sin\alpha$. The weighted length of the optimal path σ between to points $(x_1, 0)$ and $(x_2, 0)$ on a is equal to

$$L^*(\sigma) = \int_{x_1}^{x_2} \frac{1}{x \sin\alpha}\, dx$$

$$= \frac{\ln x}{\sin\alpha}\Big|_{x_1}^{x_2} = \frac{1}{\sin\alpha} \cdot \ln\frac{x_2}{x_1}. \quad (12)$$

- *Same polygon vertex–edge arc*. Without loss of generality, let the polygon vertex and the polygon edge inducing the Voronoi arc a be the origin and the line $x = 0$, respectively. Then, the Voronoi arc a is supported by the line $y = 0$, and the clearance for any point $(x, 0)$ along a is equal to x. The weighted length of the optimal path σ between to points $(x_1, 0)$ and $(x_2, 0)$ on a is equal to

$$L^*(\sigma) = \int_{x_1}^{x_2} \frac{1}{x}\, dx = \ln x|_{x_1}^{x_2} = \ln\frac{x_2}{x_1}. \quad (13)$$

- *Different polygon vertex–edge arc*. Without loss of generality, let the polygon vertex and the polygon edge inducing the Voronoi arc a be the point $(0, y_v)$ and the line $y = -y_v$, respectively. Then, the Voronoi arc a is supported by the parabola $y(x) = x^2/4y_v$, and the clearance for any point $(x, y(x))$ along a is equal to $y(x) + y_v$. The weighted length of the optimal path σ between to points $(x_1, 0)$ and $(x_2, 0)$ on a is equal to

$$L^*(\sigma) = \int_{x_1}^{x_2} \frac{\sqrt{1 + (dy/dx)^2(x)}}{y(x) + y_v}\, dx \quad (14)$$

$$= \int_{x_1}^{x_2} \frac{\sqrt{1 + x^2/4{y_v}^2}}{(x^2/4y_v) + y_v}\, dx \quad (15)$$

$$= \int_{x_1}^{x_2} \frac{2}{\sqrt{x^2 + 4{y_v}^2}}\, dx \quad (16)$$

$$= 2\ln\left(x + \sqrt{x^2 + 4{y_v}^2}\right)\Big|_{x_1}^{x_2}$$

$$= 2\ln \frac{x_2 + \sqrt{{x_2}^2 + 4{y_v}^2}}{x_1 + \sqrt{{x_1}^2 + 4{y_v}^2}}. \quad (17)$$

We conclude that an optimal path γ^* between a start position s and a goal position g amidst polygonal obstacles in the plane consists of segments of different types: spiral arcs in Voronoi cells of a polygon vertex, circular arcs in Voronoi cells of a polygon edge and pieces of Voronoi arcs on the Voronoi diagram itself. We refer to them as *maximal* path segments. We have already seen how we can compute the weighted length of each of these maximal segments. In addition, according to Lemma 2 we know that these segments are smoothly connected.

We next show that the number of maximal segments in an optimal path is linear in the complexity of the obstacles.

Lemma 9. *An optimal path γ^* consists of at most $12n$ maximal segments, where n is the total number of polygon vertices.*

Proof. We have already seen that the arcs of the Voronoi diagram are locally optimal paths. Hence, if there are two points on an arc of $\mathcal{V}$ belonging to γ^*, these points are connected by a piece of the diagram arc. For each arc a in $\mathcal{V}$, one of the following holds: (i) the optimal path γ^* does not intersect a at all; or (ii) γ^* crosses a exactly once; or (iii) γ^* contains one continuous piece of a. At the same time, the endpoints of spiral segments and circular segments must coincide with $\mathcal{V}$ (or with s or g), as they are the transition points between two segments of different types.

Using the Euler formula, it is possible to show that the number of Voronoi arcs in $\mathcal{V}$ is bounded by $6(n-1)$, where n is the total number of polygon vertices n. Note that every Voronoi arc can account for at most two maximal path segments: one path segment on the arc and one segment arriving on the arc (the path segment leaving the arc is accounted for by the arc on which it arrives). The complexity of γ^* is therefore at most $12n$. ■

So far we covered the case of a point moving amidst polygonal obstacles in the plane. If this is not the case, we can still view the moving entity as a point if we consider the configuration-space obstacles. If the robot is polygonal and can only translate, but not rotate, the configuration-space obstacles are the Minkowski sums of the original obstacles with the robot rotated by π, and are also straight-edge polygons in this case.

In the case of a disk robot of radius ρ moving amidst polygonal obstacles, we should dilate each obstacle by ρ, namely compute the Minkowski sum of each polygon with the disk, and obtain a set of polygonal configuration-space obstacles, whose boundaries comprise line segments *and* circular arcs. The analysis we performed in this section also applies for the case of moving amidst such dilated polygons. Note that in the general case the arcs of the Voronoi diagram of a set of line segments and circular arcs consists of line segments (equidistant from a pair of line segments), parabolic arcs (equidistant

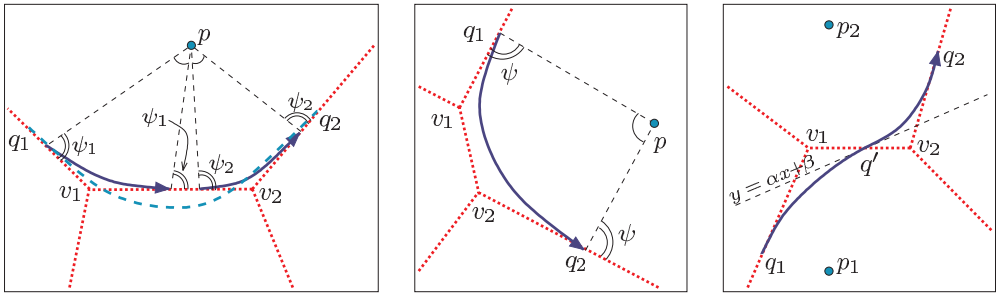

Fig. 5. Adding shortcut curves in the Voronoi diagram of point obstacles. (a) The spiral arc connecting q_1 and q_2 (dashed) crosses the Voronoi edge v_1v_2; the optimal backbone path between q_1 and q_2 therefore comprises two spiral arcs that shortcut v_1 and v_2 (solid arrows) and portions of Voronoi edges. (b) Shortcutting two adjacent Voronoi vertices v_1 and v_2 by a single spiral arc. (c) Shortcutting two Voronoi vertices by a cross-cell curve obtained from the smooth concatenation of two spiral arcs. Both arcs have a common tangent $y = \alpha x + b$, which crosses the Voronoi edge v_1v_2 at q'.

from a line segment and a circular arc) and *hyperbolic* arcs (equidistant from a pair of circular arcs). However, as all circular arcs of the dilated obstacles have the same radius in our case, the hyperbolic arcs degenerate into line segments, hence all Voronoi edges are locally optimal. The Voronoi edges subdivide the plane into cells that can either be associated with a closest dilated polygon edge (a line segment) or with a dilated polygon vertex (a circular arc). It is possible to express the optimal path between two points in a cell ζ of the latter type in a closed analytic form, using calculus of variations; see Appendix A.3 for the details.

If we have a robot of an arbitrary shape that is able to translate and rotate, namely has three degrees of motion freedom, it is sufficient in some cases to produce a conservative solution by considering a bounding disk of the robot, and planning a path for this disk, as described above.

Having characterized various segments of an optimal path amidst polygonal obstacles, we would like to construct such paths. We know that an optimal path contains portions of the Voronoi diagram, but it cannot totally overlap with the Voronoi diagram: a path retracted to a Voronoi diagram may pass through Voronoi vertices, hence it may contain sharp turns, in contradiction to Lemma 2. One may try to rectify this problem by introducing a *shortcut curve* between each pair of Voronoi edges that are incident to a common Voronoi vertex. Figure 5(a) and (b) show how we introduce shortcut curves in the Voronoi diagram of point obstacles; these simple shortcut curves pass through a single Voronoi cell of a polygon vertex, hence they are arcs of a logarithmic spiral. At the same time, a shortcut curve may cross a Voronoi edge; thus, it may comprise two spiral arcs that are smoothly joined together (see Figure 5(c)).

We should also continue to examine the possibility of shortcutting $k > 2$ Voronoi vertices by considering sequences of $(k + 1)$ contiguous Voronoi edges. This operation is not trivial, and requires solving a system of low-degree polynomial equations with $2(c + 1)$ unknowns, where c is the number of crossings between the shortcut curve and the Voronoi diagram. In some scenarios it may be possible to construct shortcuts to $\Theta(n)$ Voronoi vertices by considering sequences of $\Theta(n)$ contiguous Voronoi edges, thus the process of smoothing the path retracted from the Voronoi diagram may blow up exponentially. We therefore devise an approximation algorithm that computes paths that are arbitrarily close to the optimal path between a pair of given endpoints.

4. An ε Approximation Algorithm for Optimal Paths

Based on the results of the previous section, we show in this section how we construct an algorithm that computes an approximately optimal path between any given start and goal points amidst any given set of polygonal obstacles. We show that our algorithm produces paths which are at most ε longer (in terms of weighted length) than an optimal path, and prove efficient running time bounds expressed in terms of the value of ε.

4.1. The Algorithm

We devise an approximation algorithm to compute a near-optimal path between two endpoints s and g based on the structure of the Voronoi diagram $\mathcal{V}$ and the planar partition it induces. Given $\varepsilon > 0$, we subdivide the Voronoi arcs of $\mathcal{V}$ into small intervals of length $c(I)\varepsilon$: as ε is small, we consider the clearance of an interval I to be constant and denote it by $c(I)$.

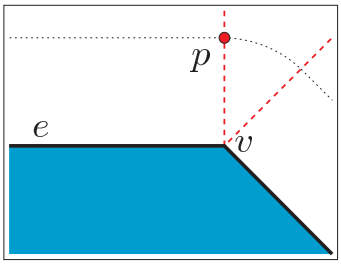

Fig. 6. The local clearance minimum cannot be attained on a Voronoi edge that separates two Voronoi cells of features of the same polygon.

Note that the intervals are shorter in regions where the clearance is smaller, and that each interval has weighted length ε.

Hence, if Λ is the total weighted length of the Voronoi arcs of $\mathcal{V}$, then there are Λ/ε intervals in total. However, the Voronoi arcs induced by two features of the same polygon have zero clearance in one of their endpoints, which would make the intervals arbitrarily small as $c(I)$ approaches zero. At the same time, Λ, the total weighted length of $\mathcal{V}$, becomes infinity.

Fortunately, we can prove that the minimal clearance of an optimal path γ^* between a start position s and a goal position g is never smaller than the minimum of the clearances attained at s, g and the Voronoi arcs of $\mathcal{V}$ induced by features of *different* polygons. As a consequence, we only need to subdivide the portions of the Voronoi diagram that have clearance greater than the minimum value, disregarding portions that are induced by features of the same obstacles and lie too close to this obstacle.

Lemma 10. *The minimal clearance of an optimal path γ^* between start position s and goal position g is greater than (or equal to) the minimum of the clearances attained at s, g, and the Voronoi arcs of V induced by features of different polygons.*

Proof. First we observe that for each of the spiral segments and circular segments of the optimal path γ^* (recall that such segments correspond to pieces of the path that are contained within a Voronoi cell of a polygon vertex or a polygon edge, respectively) the minimal clearance is attained at one of its endpoints. This means that local clearance minima along γ^* can be attained at s, g, a point where it crosses an arc of $\mathcal{V}$ and where γ^* consists of a piece of a Voronoi arc.

However, a local clearance minimum of γ^* cannot be attained at a Voronoi edge separating two Voronoi cells of features of the same polygon. Consider the scenario depicted in Figure 6, and suppose that the optimal path γ^* goes through point p on a Voronoi arc separating a Voronoi cell of a polygon vertex v and a Voronoi cell of a polygon edge e incident to this vertex. We assume, without loss of generality, that e is supported by some horizontal line. If p is a local minimum of γ^* in terms of clearance, the path should not go closer to the polygon than the dotted curve in the vicinity of p. As we know that γ^* is smooth, it has a well-defined slope at p. This slope should be strictly negative, otherwise the circular segment of γ^* on the left-hand side of p goes below the dotted line. However, this means that the spiral segment of γ^* on the right-hand side of p will go below the dotted circular arc, whose slope at p is exactly zero. Thus, p cannot be a local clearance minimum of γ^*.

We conclude that local clearance minima can only be attained at Voronoi arcs induced by features of different polygons, at s and at g. The clearance obtained along γ^* is therefore never smaller than the minimum of the clearances attained at s, g, and the Voronoi arcs of $\mathcal{V}$ induced by features of different polygons. ■

Let us now define a graph $\mathcal{D}$ whose set of nodes is equal to the set of intervals $\mathcal{I}$ plus the endpoints s and g. Each interval is incident to two of the cells defined by the Voronoi diagram, and we connect $I_1, I_2 \in \mathcal{I}$ by an edge if and only if they are incident to a common cell. This edge is a spiral arc in a Voronoi cell of one of the polygon vertices, a circular arc in a Voronoi cell of one of the polygon edges, and a straight-line segment or a parabolic arc on a Voronoi arc (depending on the type). In addition, an edge of $\mathcal{D}$ should not cross any of the arcs of $\mathcal{V}$. The endpoints s and g are connected to the graph in a similar fashion.

Having constructed $\mathcal{D}$, it is now possible to use Dijkstra's algorithm to compute a near-optimal path connecting s and g. The complete algorithm is given in pseudo-code in Algorithm 1.

4.2. Near-optimal Paths

We show that the algorithm described above indeed gives a near-optimal path. Let γ^* be the optimal path between s and g, which comprises $k < 12n$ maximal segments $\gamma_1, \ldots, \gamma_k$ (a path segment may be a spiral arc, a circular arc or a piece of a Voronoi arc). We next show that each such segment is approximated by an edge in the graph $\mathcal{D}$ we have constructed.

Lemma 11. *For each maximal segment γ_i of the optimal path γ^*, there exists an edge $\tilde{\gamma}_i$ in $\mathcal{D}$ such that $L^*(\tilde{\gamma}_i) < L^*(\gamma_i) + 2\varepsilon$.*

Proof. Let us denote the endpoints of the path segment γ_i by q_1 and q_2, and let I_1 and I_2 be the intervals that contain these endpoints, respectively.

An edge $\tilde{\gamma}_i$ connects the intervals I_1 and I_2 in $\mathcal{D}$, which is the optimal path connecting two endpoints $\tilde{q}_1 \in I_1$ and $\tilde{q}_2 \in I_2$. In particular, the weighted length of this edge is less than the weighted length of the path comprising the segment $\tilde{q}_1 q_1$ on

Algorithm 1 NEAROPTIMALPATH($s, g, \mathcal{O}, \varepsilon$)

Construct Voronoi diagram $\mathcal{V}$ of polygonal obstacles $\mathcal{O}$.
Subdivide all portions of the Voronoi arcs of $\mathcal{V}$ whose clearance is larger than the minimum clearance attained at s, g and the Voronoi arcs of $\mathcal{V}$ induced by features of different polygons into intervals I of length $c(I)\varepsilon$.
Let $\mathcal{I}$ be the set of all intervals I, plus s and g.
Construct graph $\mathcal{D}$ by connecting all pairs of intervals adjacent to a common Voronoi cell by an edge of the appropriate type if the edge does not intersect any features of $\mathcal{V}$.
for all $I \in \mathcal{I}$ **do**
  $d(I) \leftarrow \infty$.
$d(s) \leftarrow 0$.
Insert s into priority queue $\mathcal{Q}$.
while $\mathcal{Q}$ is not empty **do**
  Pop element I with minimal $d(I)$ from the queue $\mathcal{Q}$.
  if $I = g$ **then**
    Path has been found. Follow backpointers $b(I)$ to extract the path. Terminate.
  else
    for all edges $\langle I, I' \rangle$ incident to I in $\mathcal{D}$ **do**
      if $d(I') < d(I) + L^*(\langle I, I' \rangle)$ **then**
        $d(I') \leftarrow d(I) + L^*(\langle I, I' \rangle)$.
        $b(I') \leftarrow I$.
        Insert (or update) I' in $\mathcal{Q}$.
Path does not exist.

a Voronoi arc, the segment γ_i of the optimal path γ^*, and the segment $q_2\tilde{q}_2$ on a Voronoi arc. Since q_j and $\tilde{q}_j$ (for $j = 1, 2$) lie on the same interval I_j, and the length of I_j is $c(I_j)\varepsilon$, we therefore obtain

$$\begin{aligned} L^*(\tilde{\gamma}_i) &< L^*(\tilde{q}_1 q_1) + L^*(\gamma_i) + L^*(q_2\tilde{q}_2) \\ &\leq \frac{\|\tilde{q}_1 - q_1\|}{c(I_1)} + L^*(\gamma_i) + \frac{\|q_2 - \tilde{q}_2\|}{c(I_2)} \\ &\leq L^*(\gamma_i) + 2\varepsilon. \end{aligned}$$

The weighted length of the approximated segment $\tilde{\gamma}_i$ contained in $\mathcal{D}$ can therefore be at most $L^*(\gamma_i) + 2\varepsilon$. ■

Since two consecutive segments γ_i and γ_j of the optimal path both have an endpoint in a common interval, we know that the edges from $\mathcal{D}$ approximating γ_i and γ_j are connected in a common vertex of $\mathcal{D}$. Hence, the series of edges approximating each of the optimal path segments form a continuous path $\tilde{\gamma}$. This path is near-optimal.

Corollary 12. *Given a set of polygonal obstacles having n vertices in total, and given $\varepsilon > 0$, it is possible for any pair of endpoints s and g with $c(s), c(g) > 0$, to construct a graph $\mathcal{D}$ and compute a near-optimal path $\tilde{\gamma}$ connecting s and g, such that $L^*(\tilde{\gamma}) < L^*(\gamma^*) + 24n\varepsilon$.*

Alternatively, we can choose the length of the intervals to be $c(I)(\varepsilon/24n)$. In this case, a near-optimal path $\tilde{\gamma}$ can be found such that $L^*(\tilde{\gamma}) < L^*(\gamma^*) + \varepsilon$.

4.3. Running Time Analysis

Let us now analyze the running time of our algorithm. The Voronoi diagram $\mathcal{V}$ of the polygonal obstacles can be constructed in $O(n \log n)$ time. Second, we need to construct the graph $\mathcal{D}$. Using a brute-force algorithm that checks each candidate edge versus the $O(n)$ diagram arcs, $\mathcal{D}$ can be constructed in $O((\Lambda^2/\varepsilon^2)n)$ time, where Λ is the total weighted length of the Voronoi diagram $\mathcal{V}$, ignoring pieces of the diagram having clearance less than the minimal value of $c(s)$ and $c(g)$ and of the clearance attained at the Voronoi arcs of $\mathcal{V}$ induced by features of different polygons. However, it is possible to reduce the construction time by using the ray-shooting data-structure devised by Agarwal et al. (1993): We construct the ray-shooting data-structure on top of the Voronoi diagram in $O(n \log n)$ time. Each time we consider a candidate edge pq for $\mathcal{D}$, we shoot a ray from p in the direction of q, and add pq to $\mathcal{D}$ only if the query result is further than q. As each query takes $O(\sqrt{n} \log n)$ time, we can construct $\mathcal{D}$ in $O((\Lambda^2/\varepsilon^2)\sqrt{n} \log n)$ time.

Next, we execute Dijkstra's algorithm, whose running time is well known to be $O(E + N \log N)$, where E is the number of edges in the graph, and N the number of nodes. As in our case,

$$N = \frac{\Lambda}{\varepsilon} \quad \text{and} \quad E = \frac{\Lambda^2}{\varepsilon^2},$$

Dijkstra's algorithm takes $O(\Lambda^2/\varepsilon^2)$ time.

Corollary 13. *Given a set of polygonal obstacles having n vertices in total, and given $\varepsilon > 0$, it is possible for any pair of endpoints s and g with $c(s), c(g) > 0$, to compute a near-optimal path $\tilde{\gamma}$ connecting s and g with $L^*(\tilde{\gamma}) < L^*(\gamma^*) + 24n\varepsilon$ in $O(((\Lambda^2/\varepsilon^2)\sqrt{n} + n) \log n)$ time.*

Alternatively, when we choose the length of the intervals to be $c(I)(\varepsilon/24n)$, a near-optimal path $\tilde{\gamma}$ with $L^*(\tilde{\gamma}) < L^*(\gamma^*) + \varepsilon$ can be found in $O((\Lambda^2/\varepsilon^2)n^{5/2} \log n)$ time.

To give an illustration of how optimal paths for varying δ values look, we implemented a brute-force algorithm that performs an A^*-search on a dense grid. Figure 7 shows the optimal paths between a pair of points for different δ values.

5. Planning Near-optimal Corridors

In this section, we apply the results of the previous sections to *corridors*. We first formally define a corridor, and then

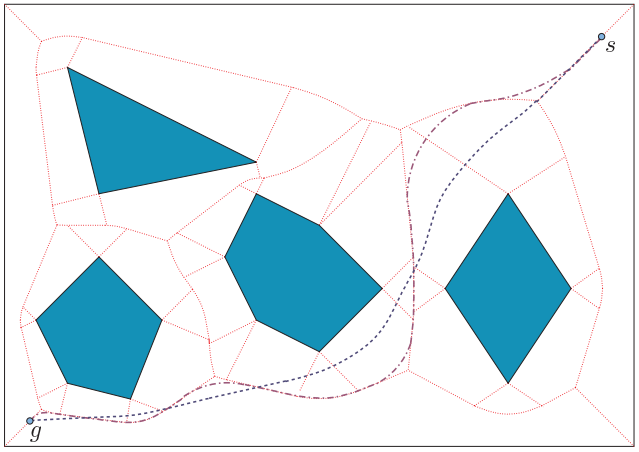

Fig. 7. Optimal paths between two locations s and g for different δ values. The thick dashed curve traces the optimal path for $\delta = \frac{1}{8}$ and the thick dash-dotted curve is the optimal path for $\delta = 1$. Note that as we increase the value of δ, the optimal path becomes more like that obtained from the Voronoi diagram of the obstacles (dotted).

show how we can characterize and compute optimal corridors. We also show how we can take into account curvature in the weighted length measure of corridors.

5.1. Corridors

A *corridor* $C = \langle \gamma(t), w(t), w_{\max} \rangle$ in a d-dimensional workspace (typically $d = 2$ or 3) is defined as the union of a set of d-dimensional balls whose center points lie along the *backbone path* of the corridor, which is given by the continuous function $\gamma : [0, L] \longrightarrow \mathbb{R}^d$. The radii of the balls along the backbone path are given by the function $w : [0, L] \longrightarrow (0, w_{\max}]$. Both γ and w are parameterized by the length of the backbone path. In the following, we refer to $w(t)$ as the *width* of the corridor at point t. The width is positive at any point along the corridor, and does not exceed $w_{\max}$, a prescribed *desired width* of the corridor.

Given a corridor $C = \langle \gamma(t), w(t), w_{\max} \rangle$ of length L in $\mathbb{R}^d$, the interior of the corridor is thus defined by $\bigcup_{t \in [0,L]} B(\gamma(t); w(t))$, where $B(p; r)$ is an open d-dimensional ball with radius r that is centered at p. The interior of the corridor should be disjoint from the interior of a given set $\mathcal{O}$ of obstacles; otherwise, it is an invalid corridor. In what follows we consider only valid corridors.

Note that if we examine the intersection of the corridor $C = \langle \gamma(t), w(t), w_{\max} \rangle$ with a $(d-1)$-dimensional hyperplane through $\gamma(t)$, whose normal is tangent to γ at $\gamma(t)$, the volume of the cut is proportional to $w^{d-1}(t)$, allowing the entities moving along the corridor less space to maneuver than in a maximally wide corridor. Thus, we wish to penalize corridor portions whose width is less than $w_{\max}$. We do this by defining the *weighted length* $L^*(C)$ of a corridor $C = \langle \gamma(t), w(t), w_{\max} \rangle$ to be

$$L^*(C) = \int_\gamma \left(\frac{w_{\max}}{w(t)} \right)^{d-1} dt. \tag{18}$$

We wish to minimize the weighted length by either shortening the backbone path or by extending the corridor's width up to $w_{\max}$. Given a start position $s \in \mathbb{R}^d$ and a goal position $g \in \mathbb{R}^d$, a corridor $C = \langle \gamma(t), w(t), w_{\max} \rangle$ satisfying $\gamma(0) = s$ and $\gamma(L) = g$ is *optimal* if for any other valid corridor C' connecting the two endpoints we have $L^*(C) \leq L^*(C')$.

It is straightforward to observe that if for some portion of the backbone path γ of a corridor C, we have $w(t) < \min\{c(\gamma(t)), w_{\max}\}$ for $t \in [t_0, t_0 + \tau]$ $(\tau > 0)$, we can improve the quality of the corridor by letting $w(t) \longleftarrow \min\{c(\gamma(t)), w_{\max}\}$ for each $t \in [t_0, t_0 + \tau]$. Given a set of obstacles and a $w_{\max}$ value, we can associate the *bounded clearance* measure $\hat{c}(p)$ with each point $p \in \mathbb{R}^d$, where $\hat{c}(p) = \min\{c(p), w_{\max}\}$. Using the observation above, it is clear that the width function of an optimal corridor $C = \langle \gamma(t), w(t), w_{\max} \rangle$ is simply given by $w(t) = \hat{c}(\gamma(t))$. We conclude that in order to plan an optimal corridor amidst a set of obstacles $\mathcal{O}$ we have to compute an optimal backbone path amidst the obstacles with respect to the clearance measure $\hat{c}(\cdot)$ bounded by the preferred corridor width $w_{\max}$. Note that the bounded clearance function is also continuous and satisfies the Lipschitz condition, hence Lemma 2 also holds for the case of corridors, namely the backbone path γ of an optimal corridor must be smooth.

5.2. Characterizing Optimal Corridors

Let us begin by considering an environment with a single point obstacle. We already know that if we are given two endpoints whose clearance is less than $w_{\max}$, then the optimal corridor connecting them is characterized by a backbone path supported by a logarithmic spiral (see Section 3.1). Let us analyze the case where the clearance of the two endpoints exceeds $w_{\max}$, namely the two endpoints of our path lie outside the closure of the disk $B(p; w_{\max})$. There are two possible scenarios: (i) the straight line segment sg does not intersect $B(p; w_{\max})$—in this case, this segment is the backbone of the optimal corridor; (ii) sg intersects $B(p; w_{\max})$—in this case the optimal backbone path is a bit more involved. Consider some backbone path γ connecting s and g. It is clear that the intersection of γ with $B(p; w_{\max})$ comprises a single component (otherwise we have a segment of the backbone path lying outside $B(p; w_{\max})$, which we can shortcut be traversing the circular arc that connects its endpoints), so we denote the point where the path enters the disk by s' and the point where it leaves the disk by g' (see Figure 8). As s' and g' lie on the disk boundary, their polar representation is $s' = w_{\max} e^{i\theta_{s'}}$ and $g' = w_{\max} e^{i\theta_{g'}}$, so

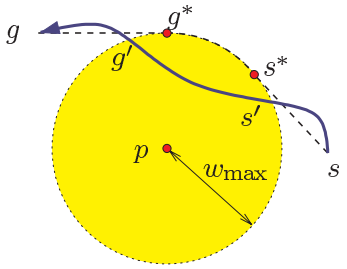

Fig. 8. The point where the path enters the disk, s', and the point where it leaves the disk, g'.

we use (3) and (4) and obtain that $a^* = w_{\max}$ and $b^* = 0$. The optimal path between s' and g' therefore lies on the degenerate spiral $r = w_{\max}$, namely the circle that forms the boundary of $B(p; w_{\max})$. We conclude that the optimal backbone path between s and g must contain a circular arc on the boundary of $B(p; w_{\max})$. Since, according to Lemma 2, this path must be smooth, it should consist of two line segments ss^* and g^*g that are tangent to the disk and a circular arc that connects the two tangency points s^* and g^* (see the dashed path in Figure 8). Note that as there are two possible tangents emanating from each endpoint, we should consider the four possible paths and select the shortest. Similarly, in cases where one endpoint (say g) is located inside $B(p; w_{\max})$ and the other outside this disk, the optimal backbone path consists of a line segment emanating from s that connects smoothly, on some point on the boundary of $B(p; w_{\max})$, to an arc of a logarithmic spiral that reaches g.

Using similar arguments it is not difficult to show that if we have a single *convex* polygonal obstacle P, we should examine whether the line segment sg intersects the dilated obstacle $P \oplus B(w_{\max})$. If it does, the optimal corridor consists of two tangents emanating from s and g to the circular arcs of the dilated polygon, with the tangency point connected by a portion of the dilated polygon boundary. In cases where P is not convex, then the optimal path contains a portion of the dilated boundary of its *convex hull*.

Let us now examine the more general scenarios of an environment cluttered with polygonal obstacles $\mathcal{O} = \{P_1, \ldots, P_m\}$. We consider the dilated obstacles $P_i \oplus B(w_{\max})$. In cases where the polygons are well separated, that is, for each $i \neq j$ the dilated obstacles $P_i \oplus B(w_{\max})$ and $P_j \oplus B(w_{\max})$ are disjoint in their interiors (implying that the distance between the two obstacles is at least $2w_{\max}$), we can follow the same arguments used above for a single obstacle and conclude that the optimal backbone path between two points s and g with $c(s), c(g) > w_{\max}$ is contained in the *visibility graph* of the dilated obstacles and of s and g.

The visibility graph of the set of dilated obstacles can be constructed in $O(n^2 \log n)$ time, n being the total complexity of the obstacles, by performing a radial sweep from each dilated vertex. If all polygonal obstacles are convex, it is possible to compute their visibility graph in $O(n \log n + E)$ time, where E is the number of visibility edges in the graph (Pocchiola and Vegter 1996). Given a path-planning query, namely two endpoints s and g, we first check whether the straight line segment sg is free. If it is, it should serve as the backbone of the corridor connecting s and g. Otherwise, we treat s and g as graph vertices and add all free tangents from s and from g to the disks as graph edges. We then perform Dijkstra's algorithm from s to find the shortest path to g in the resulting graph. Note that all edges in the graph represent line segments or circular arcs that have clearance of at least $w_{\max}$, so their weighted length is proportional to their Euclidean length.

Proposition 14. *Given a set $\mathcal{O}$ of polygonal obstacles in the plane that are well separated with respect to $w_{\max}$, and two endpoints s and g with clearance at least $w_{\max}$, it is possible to compute an optimal corridor connecting s and g in $O(E \log n)$ time using the visibility graph of the dilated obstacles, where n is the total number of obstacle vertices and E is the number of visibility edges in this graph.*

In cases where the endpoints s and g have arbitrary clearance, and the dilated obstacles are not necessarily pairwise disjoint in their interiors, let us consider the union of the dilated obstacles $\mathcal{M} = \bigcup_{i=1}^{m} (P_i \oplus B(w_{\max}))$. The boundary of $\mathcal{M}$ consists of straight-line segments (dilated obstacle edges) and circular arcs (dilated vertices). We now construct $\mathcal{V}$, the Voronoi diagram of the original obstacles, and compute the intersection $\mathcal{V} \cap \mathcal{M}$, namely the portions of the Voronoi edges contained within the union of the dilated obstacles; see Figure 9 for an illustration. The Voronoi edges, together with the arcs that form the boundary of $\mathcal{M}$, constitute the *bounded Voronoi diagram* of the obstacle set $\mathcal{O} = \{P_1, \ldots, P_m\}$, which we denote by $\hat{\mathcal{V}}(\mathcal{O})$. We refer to a point where a portion of the Voronoi edge connects to the boundary of $\mathcal{M}$ as a *connection point* of $\hat{\mathcal{V}}(\mathcal{O})$.

Note that $\hat{\mathcal{V}}(\mathcal{O})$ partitions the plane into two-dimensional cells of two types: bounded Voronoi regions of the obstacle features, and regions where the clearance is greater than $w_{\max}$. We know that if we have two endpoints s' and g' in a cell ζ whose clearance is greater than $w_{\max}$, the optimal backbone path between these endpoints is a straight-line segment, provided that $s'g'$ does not intersect any feature of $\hat{\mathcal{V}}(\mathcal{O})$. The weighted length of this segment is proportional to the Euclidean distance $\|g' - s'\|$. On the other hand, if ζ is a bounded Voronoi cell, then the optimal backbone path between s' and g' is either a spiral arc or a circular arc, provided that this arc does not intersect $\hat{\mathcal{V}}(\mathcal{O})$ (see the discussion in Section 3.3). In addition, the edges of the bounded Voronoi diagram are locally optimal.

Trying to generalize the construction of the visibility graph, it is possible to add *visibility edges* to the bounded Voronoi

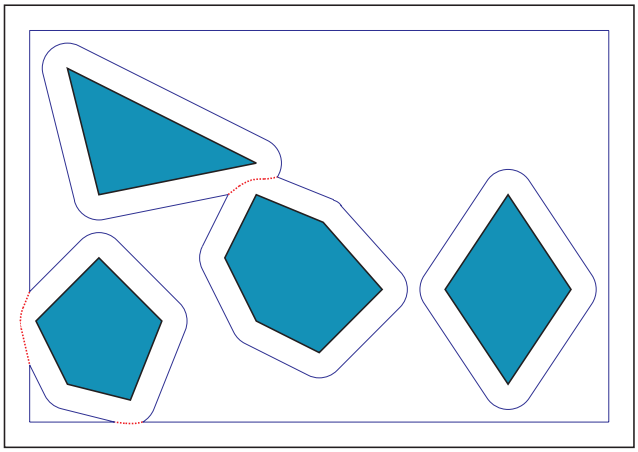

Fig. 9. The bounded Voronoi diagram of four polygons enclosed in a rectangular room. The boundary of $\mathcal{M}$, the union of the dilated obstacles, is drawn in solid lines and the Voronoi edges are dotted.

diagram, namely to consider every free bitangent of two circular arcs, every free line segment from a connection point tangent to a circular arc and every free line segment between two connection points. The resulting construct is the visibility–Voronoi diagram of the obstacles for clearance $w_{\max}$; see Wein et al. (2007) for more details. However, a path extracted from such a graph may pass through Voronoi vertices and connection points, thus it may contain sharp turns. As explained in Section 3.3, adding shortcut curves to the diagram is not feasible in many cases.

We therefore generalize the approximation algorithm presented in Section 4 to the case of planning optimal backbone paths for corridors. Instead of considering small intervals of the Voronoi diagram, we subdivide the *bounded* Voronoi diagram into intervals of length $(c(I)/w_{\max})\varepsilon$. We connect two intervals I_1 and I_2 in a similar fashion to what is described in Section 4. We note, however, that (i) if I_1 and I_2 are both incident to a cell where the clearance is greater than $w_{\max}$, we connect them by a straight line segment, and that (ii) intervals on the boundary of a dilated obstacle are connected by a line segment, or by a circular arc. In any case, it is easy to verify that Lemma 11 also holds for path segments of these types.

Corollary 15. *Given a set of polygonal obstacles $\mathcal{P}$ having n vertices in total, where $d_{\min}$ is the minimal distance between a pair of polygons in $\mathcal{P}$ (namely $\min_{P,Q\in\mathcal{P}} \operatorname{dist}(P, Q)$). Let $\overline{\Lambda}$ be the total weighted length of the bounded Voronoi diagram $\hat{\mathcal{V}}(\mathcal{P})$ with respect to a given $w_{\max}$ value, ignoring portions of the diagram having clearance less than $\frac{1}{2}d_{\min}$. Given $\varepsilon > 0$, we can construct a graph $\mathcal{D}$ over the intervals of $\hat{\mathcal{V}}(\mathcal{P})$ in $O(((\overline{\Lambda}^2/\varepsilon^2)\sqrt{n}+n)\log n)$ time, such that for each two endpoints s and g with $c(s), c(g) > \frac{1}{2}d_{\min}$, it is possible use $\mathcal{D}$ and compute a near-optimal backbone of a corridor C connecting s and g in $\tilde{O}(\overline{\Lambda}^2/\varepsilon^2 + n)$ time. Here $L^*(C)$ is at most $O(n)\varepsilon$ more than the weighted length of the optimal corridor connecting s and g.*

Figure 10 shows a near-optimal backbone path in an environment cluttered with polygonal obstacles. The path was computed using a brute-force approximation algorithm, performing an A*-search on a fine grid discretizing the environment. It can also be observed that a very similar path can be extracted from the visibility graph of the bounded Voronoi diagram of the obstacles. Such a path can be efficiently computed using the software described by Wein et al. (2007).

5.3. Accounting for the Corridor Curvature

In some applications having a winding backbone path decreases the quality of the corridor (see, e.g., Mitchell and Polishchuk (2007)). In the group-motion application (Kamphuis and Overmars 2004), for example, when the entities move along a straight line, they can all move at the maximal possible speed. Assume that the backbone path is a circular arc and the corridor width is w, such that it is bounded by two concentric circular arcs. The entities moving along the outer arc in this case have to take a longer route, so even if we let them move at maximal speed, the other entities have to move at a lower speed and the time it takes the group to traverse such a path increases.

5.3.1. Augmenting the Weighted-length Measure

Assume that the backbone path γ is smooth and let $\kappa(t)$ be the curvature of γ at time t. We can subdivide the path into infinitesimally small segments, such that the length of the ith path segment is ℓ_i (with $\sum_i \ell_i = L$), the width of each segment, denoted by w_i, is assumed constant and the curvature is also assumed constant and denoted by κ_i; see Figure 11 for an illustration. Hence, each path segment can be considered as a circular arc whose radius is $r_i = 1/\kappa_i$ and defined by the angle $\alpha_i = \ell_i/r_i$. The length of the outer boundary of the corridor along the ith path segment is given by $\alpha_i(r_i + w_i)$, and we can thus bound the length of each of the corridor boundary curves by

$$\begin{aligned}\sum_i \alpha_i(r_i+w_i) &= \sum_i \frac{\ell_i}{r_i}(r_i+w_i)\\ &= \sum_i \ell_i + \sum_i \frac{w_i}{r_i}\ell_i = L + \sum_i w_i\kappa_i\ell_i.\end{aligned}$$

We therefore wish to augment the weighted length function by adding a penalty for the extra length induced by the curvature

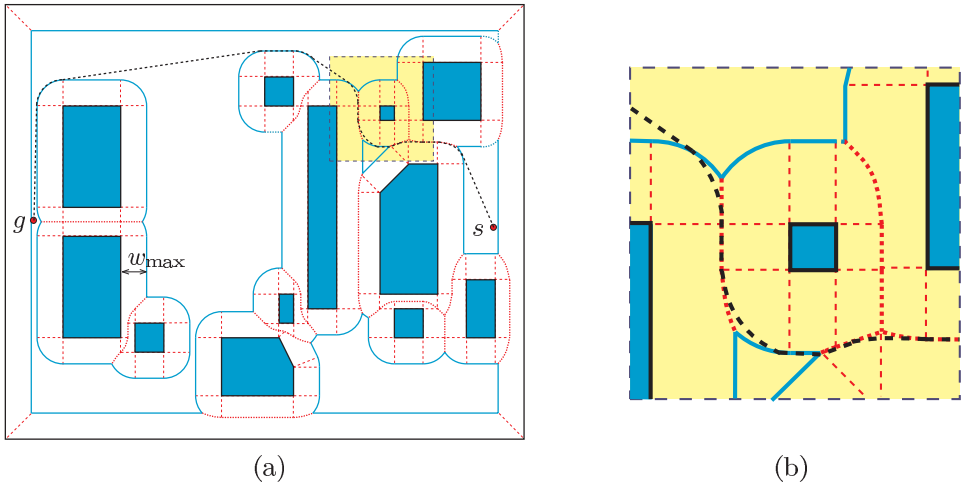

Fig. 10. (a) A near-optimal backbone path (dashed) amidst polygonal obstacles, overlayed on top of the bounded Voronoi diagram of the obstacles. Boundary edges are drawn in light solid lines, Voronoi chains between polygons are dotted, and Voronoi edges that separate cells of adjacent polygon features are drawn with a light dashed line. (b) Zooming in on a portion of the path; note the shortcuts the path takes.

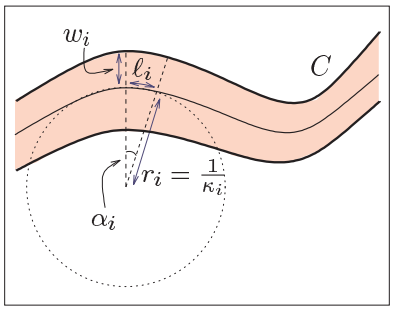

Fig. 11. Subdivision of the path into infinitesimally small segments, such that the length of the ith path segment is ℓ_i (with $\sum_i \ell_i = L$), the width of each segment, denoted by w_i, is assumed constant and the curvature is also assumed constant and denoted by κ_i.

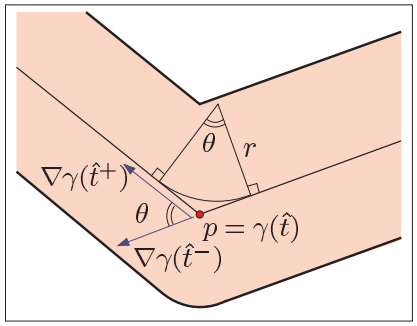

Fig. 12. Replacing a sharp turn in the backbone path by a smooth circular arc.

of the backbone path, which is equal to $\sum_i w_i \kappa_i \ell_i$. However, as we can make our path segments infinitesimally small, and as γ is parameterized by its length, we can simply redefine our weighted length function for $C = \langle \gamma(t), w(t), w_{\max} \rangle$ to be

$$L^*_\mu(C) = \int_\gamma \left(\frac{w_{\max}}{w(t)} \right)^{d-1} dt + \mu \int_\gamma w(t)\kappa(t)\, dt, \qquad (19)$$

where $\mu > 0$ is the weight we give to the curvature measure. Typically, $\mu \leq 1$ as we do not wish to give more weight to the curvature than to the length or to the clearance of the backbone path.

We also wish to account for backbone paths that contain sharp turns, and are only *piecewise* $\mathcal{C}_2$-continuous; thus, the curvature of γ is not defined at a finite number of points. Let $p = \gamma(\hat{t})$ be such a point, and let θ be the angle between $\nabla\gamma(\hat{t}^-)$ and $\nabla\gamma(\hat{t}^+)$. Let us replace the sharp turn with a circular arc a of a small radius r. The arc is defined by the angle θ (see Figure 12), so its length is θr (θ is measured in radians). If r is small enough, we can assume that the corridor has a fixed width $w_p = w(\hat{t})$ over the circular arc, so we have

$$\lim_{r\to 0} \int_a w(t)\kappa(t)\, dt = \lim_{r\to 0} \int_a \frac{w_p}{r}\, dt = \lim_{r\to 0} \theta r \cdot \frac{w_p}{r} = \theta w_p.$$

We can thus abuse the curvature-integral notation, as appears in (19), and account for sharp turns by adding the dis-

crete weight as explained above. We note, however, that backbone paths of optimal corridors with respect to the augmented weighted-length measure, as defined in (19), should be smooth and cannot contain sharp turns. To see why, we can follow the proof of Lemma 2, and assume that we have an optimal backbone path γ^* that contains a sharp turn, defined by the angle θ. In the original proof we show that it is always possible to shortcut the sharp turn by a circular arc that decreases the weighted length of the path. While the original path makes a sharp turn of θ radians, the shortcut also makes the same turn, but "spreads" it over the entire arc, which contains points with less clearance. The curvature penalty we give the circular shortcut is thus smaller than the penalty of the original path, so our circular shortcut decreases the augmented weighted length of the path. We conclude that a sharp turn is not possible in an optimal corridor also when we take the curvature into account.

5.3.2. Moving Amidst Well-separated Obstacles

We are given a set $\mathcal{P}$ of obstacles (point obstacles or polygonal obstacles) in the plane, and preferred width $w_{\max}$, such that the obstacles of $\mathcal{P}$ are well separated with respect to $w_{\max}$. Given two query points $s, g \in \mathbb{R}^2$ whose clearance value is at least $w_{\max}$, we would like to compute the backbone path connecting s and g that induces an optimal corridor with respect to the augmented measure L^*_μ.

In Section 5.2 we showed that such an optimal path is contained in the visibility graph of the dilated obstacles for the special case where $\mu = 0$. We next show that the same holds also for any $\mu > 0$.

Recall that a path extracted from the visibility graph of the dilated obstacles consists of line segments and circular arcs of radius $w_{\max}$. Path segments of the former type do not contribute to the curvature measure of the backbone path, where a circular arc supported by an angle α has a constant curvature of $1/w_{\max}$. The contribution of such an arc to the curvature component of the weighted length of the path is therefore $\mu\alpha w_{\max}$. If we try to shortcut the circular arc by a curve that lies closer to the obstacle, the curvature component of such a shortcut will be at least $\mu\alpha w_{\max}$, as we make an overall turn of α radians, and the weighted length of this curve will necessarily be larger than that of the original circular arc (which we know to be locally optimal in the case of $\mu = 0$). We conclude that we cannot shortcut the circular arcs.

At the same time, it is not recommended to take wider turns. Consider the example depicted in Figure 13, where the corridor C' has a longer backbone path than the corridor C extracted from the visibility graph of the dilated polygons. Since both corridors are of maximal width, it is clear that its width integral is also greater. However, the curvature integral of each the corridors is proportional to the sum of the angles defining the circular arcs, so it is obvious that the curvature integral of C' is greater than that of C, as $\alpha'_1+\alpha'_2 > \alpha_1+\alpha_2$. It is therefore clear that $L^*_\mu(C) < L^*_\mu(C')$ for each $\mu > 0$.

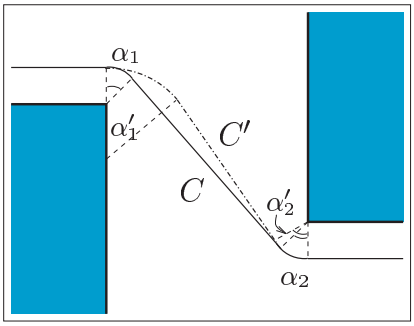

Fig. 13. The weighted length of the corridor C is larger than the weighted length of the corridor C extracted from the visibility graph of the dilated polygons.

6. Conclusions and Future Work

In this paper we have laid some theoretical foundations for measuring the quality of paths and corridors. Having introduced a measure for the quality of motion paths and studying the structure of optimal paths amidst polygonal obstacles in the plane, we show how a backbone path for an optimal corridor must look. We have also devised an approximation algorithm for computing near-optimal paths and corridors amidst obstacles.

We are currently investigating methods to speed up our approximation algorithm, as well as design simple practical methods to compute high-quality corridors.

Acknowledgements

This work has been supported in part by the IST Programme of the EU as Shared-cost RTD (FET Open) Projects under Contracts numbers IST-2001-39250 (MOVIE—Motion Planning in Virtual Environments) and IST-006413 (ACS—Algorithms for Complex Shapes), by the Israel Science Foundation (grant number 236/06), and by the Hermann Minkowski–Minerva Center for Geometry at Tel-Aviv University.

The authors wish to thank Gert Vegter for valuable comments on the contents of the paper.

Appendix A. Using Calculus of Variations for Computing Optimal Paths

We can solve the problem of computing an optimal path in the vicinity of a single obstacle using tools available from the theory of *calculus of variations*[3], a field of mathematics that deals with *functionals*, namely functions of functions, aiming

3. See, e.g., http://en.wikipedia.org/wiki/Calculus_of_variations.

to minimize the integrals of such functionals. Recall that we wish to minimize the weighted length of a path γ, which is the unknown function in this case. The weighted length is given by

$$L^*_\delta(\gamma) = \int_\gamma \left(\frac{1}{c(\gamma(t))}\right)^\delta dt = \int_0^L \frac{\|\gamma'(t)\|}{c^\delta(\gamma(t))}\, dt. \qquad (20)$$

In other words, $L^*_\delta(\gamma) = \int_0^L F(t, \gamma, \gamma')\, dt$, where the functional F is defined as $\|\gamma'(t)\|/c^\delta(\gamma(t))$. We know that the path must be smooth, hence it has two continuous derivatives. A function γ that minimizes the integral of F must therefore satisfy the Euler–Lagrange equation:

$$\frac{d}{dt}\frac{\partial F}{\partial \gamma'} = \frac{\partial F}{\partial \gamma}. \qquad (21)$$

For background material, the reader is referred to one of the numerous textbooks on the calculus of variations, for example Gelfand and Fomin (2000).

We already know that the optimal path comprises maximal segments, where each path segment lies inside a Voronoi cell. We next show how we use the Euler–Lagrange equation to express the optimal path in the vicinity of a single obstacle.

A.1. Moving Near a Point Obstacle

Let us imagine we are located in a Voronoi cell of a point obstacle (or a polygon vertex for that matter), which, without loss of generality, is located at the origin. We express our path using polar representation, so the clearance of each point along the path from $s = r_s e^{i\theta_s}$ to $g = r_g e^{i\theta_g}$ is simply its distance from the origin. We therefore look for $r = r(\theta)$ minimizing

$$L^*_\delta(\gamma) = \int_{\theta_s}^{\theta_g} \frac{1}{r^\delta(\theta)} \sqrt{r^2(\theta) + \left(\frac{dr}{d\theta}\right)^2(\theta)}\, d\theta. \qquad (22)$$

If we let $r' = dr/d\theta$ we obtain that our functional is of the form $F(\theta, r, r') = (1/r^\delta)\sqrt{r^2 + (r')^2}$. We can therefore derive this functional and obtain the following:

$$\begin{aligned}
\frac{\partial F}{\partial r} &= -\frac{\delta}{r^{\delta+1}}\sqrt{r^2 + (r')^2} + \frac{2r}{2r^\delta\sqrt{r^2 + (r')^2}} \\
&= \frac{(1-\delta)r^2 - \delta(r')^2}{r^{\delta+1}\sqrt{r^2 + (r')^2}}, \\
\frac{\partial F}{\partial r'} &= \frac{r'}{r^\delta\sqrt{r^2 + (r')^2}}, \\
\frac{d}{d\theta}\frac{\partial F}{\partial r'} &= \frac{(r''r^\delta - \delta(r')^2 r^{\delta-1})(r^2 + (r')^2) - r'r^\delta(rr' + r'r'')}{r^{2\delta}(r^2 + (r')^2)^{3/2}}.
\end{aligned}$$

Applying the Euler–Lagrange equation on the above, we obtain that $r(\theta)$ is the solution of the following regular differential equation:

$$r''(\theta)r(\theta) - (r')^2(\theta) = (1-\delta)(r(\theta) + (r')^2(\theta)). \qquad (23)$$

Note that in the special case of $\delta = 1$, the equation above reduces to the form $r''(\theta)r(\theta) = (r')^2(\theta)$. Indeed, the logarithmic spiral $r(\theta) = ae^{b\theta}$ satisfies this equation for constants a and b, that depend on the path endpoints s and g.

The solution of (23) in the general case of $\delta \neq 1$ is given by

$$r(\theta) = a\cos^{1/(\delta-1)}((\delta-1)\theta + \varphi), \qquad (24)$$

for constants a and φ. These constants can be computed by applying the constraint that the endpoints $s = r_s e^{i\theta_s}$ and $g = r_g e^{i\theta_g}$ both satisfy (24). We also note that in the special case of $\delta = 2$ we obtain the equation of the limaçon[4] $r(\theta) = a\cos(\theta + \varphi)$, which is a circle passing through the origin.

A.2. Moving Near a Line Obstacle

In cases where our path segment is in a Voronoi cell of a polygon edge, we can assume, without loss of generality, that this edge is supported by the line $y = 0$. In this case, if we express our path using Cartesian coordinates, the clearance of each point along the path from $s = (x_s, y_s)$ to $g = (x_g, y_g)$ is given by its y-coordinate. We therefore look for $y = y(x)$ minimizing

$$L^*_\delta(\gamma) = \int_{x_s}^{x_g} \frac{1}{y^\delta(x)} \sqrt{1 + \left(\frac{dy}{dx}\right)^2(x)}\, dx. \qquad (25)$$

If we let $y' = dy/dx$ we obtain that our functional is of the form $F(x, y, y') = (1/y^\delta)\sqrt{1 + (y')^2}$. Deriving this functional we obtain

$$\begin{aligned}
\frac{\partial F}{\partial y} &= -\frac{\delta}{y^{\delta+1}}\sqrt{1 + (y')^2}, \\
\frac{\partial F}{\partial y'} &= \frac{y'}{y^\delta\sqrt{1 + (y')^2}}, \\
\frac{d}{dx}\frac{\partial F}{\partial y'} &= \frac{y''y^\delta - \delta(y')^2 y^{\delta-1}(1 + (y')^2)}{y^{2\delta}(1 + (y')^2)^{3/2}}.
\end{aligned}$$

Applying the Euler–Lagrange equation on the above, we obtain that $y(x)$ is the solution of the following regular differential equation:

$$y''(x)y(x) + \delta(y')^2(x) + \delta = 0. \qquad (26)$$

It is not difficult to verify that the equation of a circular arc whose center $(x_0, 0)$ lies on the line obstacle, namely $y(x) = \sqrt{R^2 - (x - x_0)^2}$, satisfies (26) above for the special case of $\delta = 1$.

4. See, e.g., http://mathworld.wolfram.com/Limacon.html.

A.3. Moving Near a Circular Obstacle

Using similar methods, it is also possible to compute the optimal path in the vicinity of a circular obstacle of a given radius ρ. As mentioned in Section 3.3, this problem is not only interesting in its own right, but also important for computing optimal paths for a disk robot of radius ρ, where we consider a path for a point robot amidst dilated obstacles.

As we did in Section A.1, we seek a polar representation of the path. To simplify our analysis, we focus on the case of $\delta = 1$; the analysis for other δ values is quite similar. Assuming that the circular obstacle is centered at the origin, we have

$$L^*_\delta(\gamma) = \int_{\theta_s}^{\theta_g} \frac{1}{r(\theta)-\rho}\sqrt{r^2(\theta)+(r')^2(\theta)}\,d\theta. \qquad (27)$$

We now derive $F(\theta, r, r') = 1/(r-\rho)\sqrt{r^2+(r')^2}$ and obtain

$$\frac{\partial F}{\partial r} = -\frac{(r')^2+\rho r}{(r-\rho)^2\sqrt{r^2+(r')^2}},$$

$$\frac{\partial F}{\partial r'} = \frac{r'}{(r-\rho)\sqrt{r^2+(r')^2}},$$

$$\frac{d}{d\theta}\frac{\partial F}{\partial r'} = \frac{(r''(r-\rho)-(r')^2)(r^2+(r')^2)-(r')^2(r-\rho)(r+r'')}{(r-\rho)^2(r^2+(r')^2)^{3/2}}.$$

Applying the Euler–Lagrange equation on the above, we obtain that $r(\theta)$ is the solution of the following regular differential equation:

$$(r''(\theta)r(\theta)-(r')^2(\theta))(r(\theta)-\rho) = \rho(r(\theta)+(r')^2(\theta)). \quad (28)$$

A solution to (28) is given by (a and b are constants, determined by the endpoints of the curve):

$$r(\theta) = ae^{b\theta} + \frac{b^2+1}{b^2}\left(1+\frac{\rho}{4ab^2}e^{-b\theta}\right)\cdot\rho. \qquad (29)$$

We note that for $\rho = 0$, namely a point obstacle, we obtain the well known logarithmic spiral $r(\theta) = ae^{b\theta}$.

References

Agarwal, P. K., van Kreveld, M. and Overmars, M. (1993). Intersection queries in curved objects. *Journal of Algorithms*, **15**(2): 229–266.

Choset, H., Lynch, K. M., Hutchinson, S., Kantor, G., Burgard, W., Kavraki, L. E. and Thrun, S. (2005). *Principles of Robot Motion: Theory, Algorithms, and Implementations*. Boston, MA, MIT Press.

Gelfand, I. M. and Fomin, S. V. (2000). *Calculus of Variations*. New York, Dover.

Gray, A. (1997). Logarithmic spirals. *Modern Differential Geometry of Curves and Surfaces with Mathematica*, 2nd edn. CRC Press, Boca Raton, FL, pp. 40–42.

Kamphuis, A. and Overmars, M. H. (2004). Motion planning for coherent groups of entities. *Proceedings of the IEEE International Conference Robotics and Automation (ICRA)*, pp. 3815–3822.

Kamphuis, A., Pettre, J., Overmars, M. H. and Laumond, J.-P. (2005). Path finding for the animation of walking characters. *Proceedings of Eurographics/ACM SIGGRAPH Symposium on Computer Animation*, pp. 8–9.

Kavraki, L. E., Švestka, P., Latombe, J.-C. and Overmars, M. H. (1996). Probabilistic roadmaps for path planning in high-dimensional configuration spaces. *IEEE Transactions on Robotics and Automation*, **12**: 566–580.

Khatib, O. (1986). Real-time obstacle avoidance for manipulators and mobile robots. *The International Journal on Robotics Research*, **5**(1): 90–98.

Latombe, J.-C. (1991). *Robot Motion Planning*. Boston, MA, Kluwer Academic.

Lee, D.-T. and Drysdale, R. L. III (1981). Generalization of Voronoi diagrams in the plane. *SIAM Journal on Computing*, **10**(1): 73–87.

Mitchell, J. S. B. and Papadimitriou, C. H. (1991). The weighted region problem: Finding shortest paths through a weighted planar subdivision. *Journal of the ACM*, **38**(1): 18–73.

Mitchell, J. S. B. and Polishchuk, V. (2007). Thick noncrossing paths and minimum-cost flows in polygonal domains. *Proceedings of the 23rd Symposium on Computational Geometry (SCG)*, pp. 56–65.

Mitchell, J. S. B. (2004). Shortest paths and networks. *Handbook of Discrete and Computational Geometry*, 2nd edn, Goodman, J. E. and O'Rourke, J. (eds). London, Chapman & Hall/CRC, pp. 607–642.

Nieuwenhuisen, D. and Overmars, M. H. (2004). Motion planning for camera movements. *Proceedings of the IEEE International Conference on Robotics and Automation (ICRA)*, pp. 3870–3876.

Nieuwenhuisen, D. and Overmars, M. H. (2004). Useful cycles in probabilistic roadmap graphs. *Proceedings of the IEEE International Conference on Robotics and Automation (ICRA)*, pp. 446–452.

Nieuwenhuisen, D., Kamphuis, A., Mooijekind, M. and Overmars, M. H. (2004). Automatic construction of roadmaps for path planning in games. *Proceedings of the International Conference on Computer Games: Artificial Intelligence, Design and Education*, pp. 285–292.

Ó'Dúnlaing, C. and Yap, C. K. (1985). A "retraction" method for planning the motion of a disk. *Journal of Algorithms*, **6**: 104–111.

Overmars, M. H. (2005). Path planning for games. *Proceedings of the 3rd International Game Design and Technology Workshop (GDTW 2005)*, pp. 29–33.

Pocchiola, M. and Vegter, G. (1996). The visibility complex. *International Journal of Computational Geometry and Applications*, **6**(3): 279–308.

Reif, J. and Wang, H. (1995). Social potential fields: a distributed behavioral control for autonomous robots. *Proceedings of the International Workshop on Algorithmic Foundations of Robotics (WAFR)*, Goldberg, K., Halperin, D., Latombe, J.-C. and Wilson, R. (eds). Wellesley, MA, A. K. Peters, pp. 431–459.

Rimon, E. and Koditschek, D. E. (1992). Exact robot navigation using artificial potential fields. *IEEE Transactions on Robotics and Automation*, **8**: 501–518.

Russel, S. and Norvig, P. (2002). *Artificial Intelligence: A Modern Approach*, 2nd edn. Englewood Cliffs, NJ, Prentice Hall.

Sharir, M. (2004). Algorithmic motion planning. *Handbook of Discrete and Computational Geometry*, 2nd edn, Goodman, J. E. and O'Rourke, J. (eds). London, Chapman & Hall/CRC, pp. 1037–1064.

Song, G., Miller, S. and Amato, N. M. (2001). Customizing PRM roadmaps at query time. *Proceedings of the IEEE International Conference on Robotics and Automation (ICRA)*, pp. 1500–1505.

Wein, R., van den Berg, J. P. and Halperin, D. 2007. The visibility–Voronoi complex and its applications. *Computational Geometry: Theory and Applications*, **36**(1): 66–87.